Solar Energy Materials & Solar Cells 128 (2014) 204–214

Contents lists available at ScienceDirect

Solar Energy Materials & Solar Cells

journal homepage: www.elsevier.com/locate/solmat

Improvement and experimental validation of a simple behavioural model for photovoltaic modules

Badia Amrouche

CDER, Centre de Développement des Energies Renouvelables, BP 62, Route de l'Observatoire, Bouzaréah, Algiers, Algeria

ARTICLE INFO

Article history:
Received 10 February 2014
Received in revised form
13 May 2014
Accepted 13 May 2014

Keywords:
Photovoltaic module
Behavioural model
Polycrystalline silicon
Monocrystalline silicon
CdTe
CIS

ABSTRACT

The purpose of this work is to: 1) improve a previously developed behavioural model (B-model) for photovoltaic modules and 2) validate it using experimental data. The major advantages of the new model are its simplicity and the fact that it is based only on the module's electrical properties available on the manufacturer's datasheet. At first, the original model was developed and validated using a rich experimental database solely for a polycrystalline silicon photovoltaic module. However, an improved version of this model along with validation tests which use a larger database is presented in this paper. The larger database utilises the measured *I–V* characteristics of three other photovoltaic technologies such as, monocrystalline silicon, CIS and CdTe. To permit a sound and relatively easy entry into the study of photovoltaic for novices and newcomers, a detailed flowchart and description of its use are presented. Also a concrete example of an application using the flowchart is presented to display its efficiency and ease of use.

1. Introduction

Today, the importance of numerical simulation cannot be denied as well as its spinoff effects on numerous fields. This is especially true for research and industry. Numerical simulation is an indispensable experimentation tool as it permits the study of individual units, systems, phenomena, and projects in a relatively short time frame, without risk and at lower costs. It is clear that the accuracy and the reliability of numerical simulations depend on the efficiency of the models and methods used. This explains the continued infatuation for numerical development tools in many areas. The renewable energy field, especially photovoltaic, does not escape this rule.

Much research has been conducted and published on different topics in relation to PV modelling. The following studies do not comprise an exhaustive list of PV module/solar cell modelling topics and are provided as examples. Solar cells and PV modules modelling are still generating considerable interest with the aim to develop new materials/processes and solar cells/PV modules with higher conversion ratios at lower costs. Most of the work undertaken in this research axe can have one of the following aims: new PV material modelling [1–3]; solar cell modelling [4–11]; PV module modelling and characterisation [12–19]; PV module efficiency and energy rating [20–22]; and the study, analysis, and modelling of different factors which influence PV module and solar cell behaviour over their lifetime [23,24]. Many other components of PV systems have been studied, described, modelled, and simulated in a large number of research papers. For example, inverter [25–28], batteries [29–31], or motor–pump subsystem [32–34].

The photovoltaic array is the first component placed at the input of the PV conversion chain, since it assures the conversion of the sun irradiance to electricity. Because of this, it is obvious that its model is one of the “must have” tools to achieve any numerical simulation of photovoltaic systems and projects. Several models for PV arrays and modules have been developed to determine the exact current and voltage relationship. The most important differences existing amongst them are their degree of complexity and their efficiency. Many papers [35,36] present a detailed and rich state-of-the art of the existing models for PV modules and arrays.

Designers and students need a reliable and a simple tool to simulate photovoltaic modules input–output behaviours under all conditions to expeditiously complete their projects and studies. Typically, only the datasheets provided by the modules' manufacturers are available. However, these datasheets describe the devices' electric properties under only one working condition, the standard test conditions (STCs). The main objective of this project is to present and validate an improved version of the previously developed and presented behavioural model (B-model) for photovoltaic modules [37]. The major advantages of this improved model are its simplicity and the fact that it is based only on the module's electrical properties available on the manufacturer's datasheet. The previous model was originally

E-mail addresses: amrouche_badia@yahoo.fr, b.amrouche@cder.dz

http://dx.doi.org/10.1016/j.solmat.2014.05.031
0927-0248/

developed and validated using a rich experimental database only for polycrystalline silicon photovoltaic modules. Expanded validation tests are presented in this report using measured *I–V* characteristics for three other photovoltaic technologies: monocrystalline silicon, copper indium diselenide (CIS) and cadmium telluride (CdTe). To prove its efficiency, an example of its use is provided. Also, a detailed flowchart and description of its use are presented allowing a sound beginning for novices and newcomers in photovoltaic design/research.

The remainder of this paper is organised as follows: Section 2 addresses the model's fundamental principles, properties and mathematical expressions. Section 3 presents the model's improvements and instructions for use. Section 4 describes the database used which contains the measured *I–V* characteristics of three modules, monocrystalline silicon, CIS and CdTe, and presents the validation test using the measured database. Section 5 outlines a concrete example of the use of the B-model. Finally, Section 6 summarises the main results obtained and conclusions.

2. Presentation of the behavioural model

The B-model was first presented in [37]. It is a simple model for photovoltaic modules based only on the electric parameters provided by the manufacturers and available on their datasheets. The relationship between voltage and current is based on the mathematical expression of the first order system step response. However, the improved model can simulate the output electric characteristics for PV modules under any working condition by choosing ambient temperature and solar irradiance values which are expressed in Eq. (1), with: I being the modules' current; V_{oc} the open circuit voltage; I_{sc} the short circuit current; τ the voltage constant which determines the *I–V* curve's evolution at and near its maximum power point [37]; and V being the operating voltage

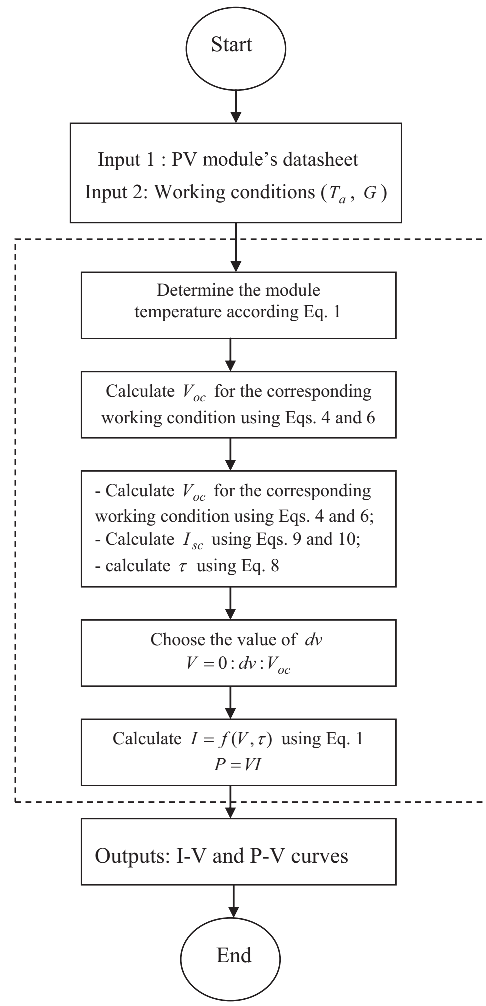

Fig. 2. B-model's instructions for use.

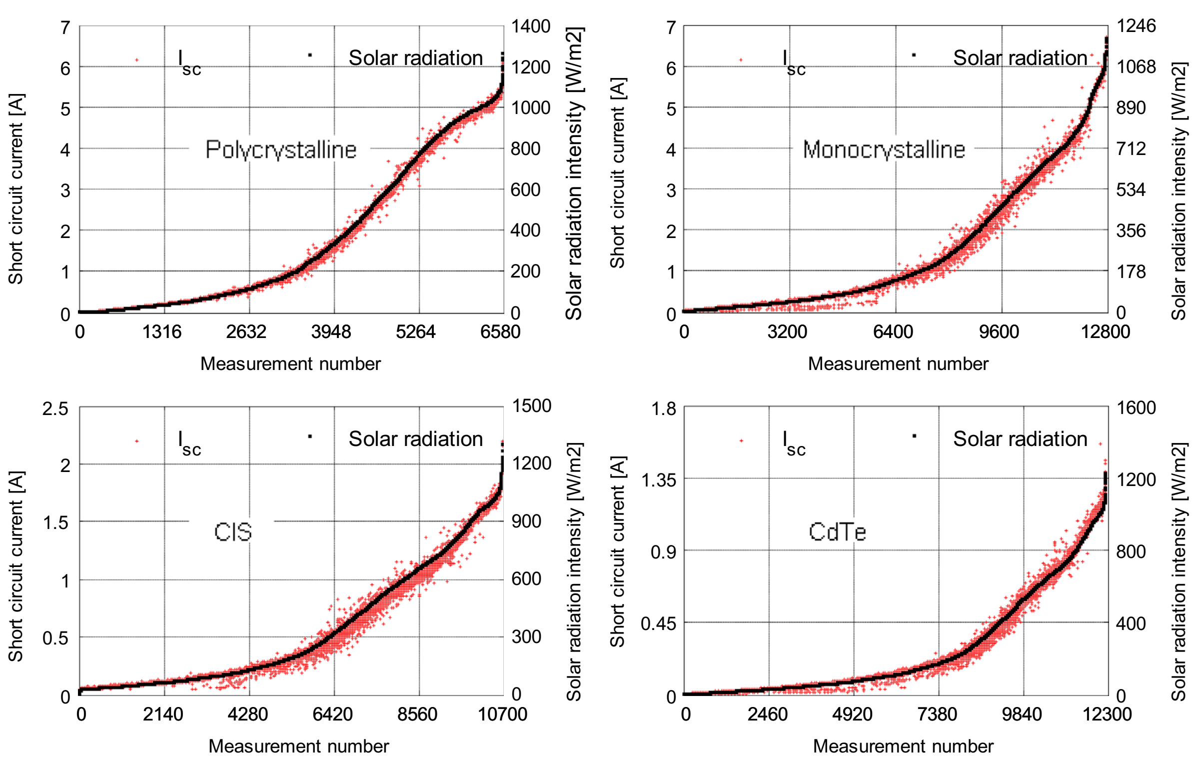

Fig. 1. The measured solar radiation intensity and the corresponding short circuit current [38].

varying between 0 and V_{oc}.

$$I(V) = \frac{I_{sc}}{1-e^{(-V_{oc}/\tau)}}\left(1-e^{(V-V_{oc})/\tau}\right) \tag{1}$$

Each working condition is characterised by a unique and specific *I*–*V* curve, and thus by a unique triplet (I_{sc}, V_{oc}, τ). These values can be calculated using Eqs. (2–8) with G being the solar irradiance (W/m^2); T the module temperature (°C); T_a the ambient temperature (°C); τ_V the rate of change for the voltage (V); τ_i the rate of change for the current (A); V_{mpp} the voltage at maximum power point; *NOCT* the Nominal Operating Cell Temperature (°C) available on the modules' datasheet along with TC_v (V/°C or %/°C), TC_i (V/°C or %/°C), and TC_{Vmpp} (V/°C or %/°C) which are the temperature coefficients of the open circuit voltage, the short circuit current, and the MPP voltage, respectively.

$$T = T_a + \frac{G}{800}(NOCT-20) \tag{2}$$

$$\tau_i(T) = 1 + \frac{TC_i}{100\%}(T-NOCT) \tag{3}$$

$$\tau_V(T) = TC_V(T-NOCT) \tag{4}$$

$$I_{sc} = \frac{G}{G_{STC}} I_{sc\_STC}\tau_i \tag{5}$$

$$V_{oc} = V_{oc\_STC} + \tau_V \tag{6}$$

Table 1
The properties of the experimental database.

PV modules	Technology	Number of *I–V* characteristics	Measuring time's duration (days)	Number of *I–V* curves used for the present validation
Mod1	Mono-crystalline	12,755	135	966
Mod2	CIS	10,701	131	1042
Mod3	CdTe	12,250	131	935

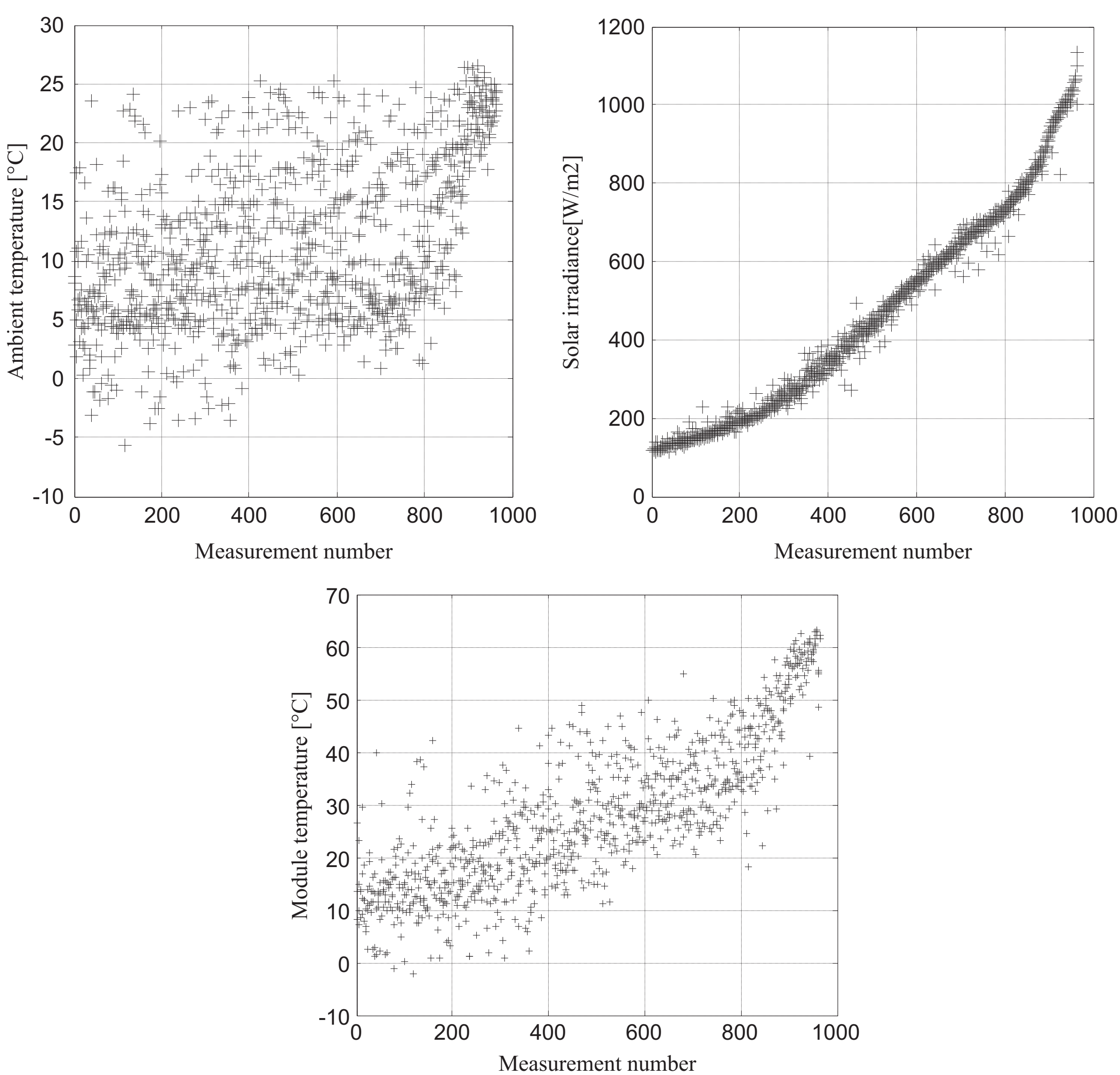

Fig. 3. Validation data of the monocrystalline silicon module.

$$\tau = \frac{V_{oc} - V_{mpp}}{2.16} \tag{7}$$

$$\tau = \frac{(V_{oc\_STC} - V_{mpp\_STC}) + (T - NOCT)(TC_V - TC_{Vmpp})}{2.16} \tag{8}$$

3. The model's improvement and the description of its instructions for use

According to the findings of a previous study [38], in which approximately 42,000 measured electrical output characteristics of PV modules with four different technologies have been analysed, a proportional correlation exists between the short circuit current and the corresponding solar irradiance intensity. This correlation, shown by Fig. 1, can be simplified as noted by Eq. (9), with G being the solar irradiance and k being a proportionality constant which can be defined using the datasheet's information as described by Eq. (10). Thus, Eqs. (3) and (5) can be substituted by Eq. (9).

$$I_{sc} = kG \tag{9}$$

$$k = \frac{I_{sc\_STC}}{G_{STC}} \tag{10}$$

The I–V and P–V electrical characteristics for any PV module can be determined according to the flowchart shown in Fig. 2. The model's inputs are the working conditions (the solar irradiance intensity and the ambient temperature) along with the electrical properties of the PV module. The outputs of the model are the current–voltage and the power–voltage characteristics. The user must utilise the information provided by the module's manufacturer and available on its datasheet.

4. The experimental validation of the B-model

In this section, the applicability of the developed model for other technologies is discussed and the results of its validation test are presented. For this, three PV modules from different technologies were considered; monocrystalline silicon, CIS, and CdTe with the understanding that the model was first developed using polycrystalline silicon module's measured database. These are the same modules used in the previous study [38]. The four modules have been characterised at the French National Institute of Solar Energy (INES) using the methods described previously [39] and the I–V curve

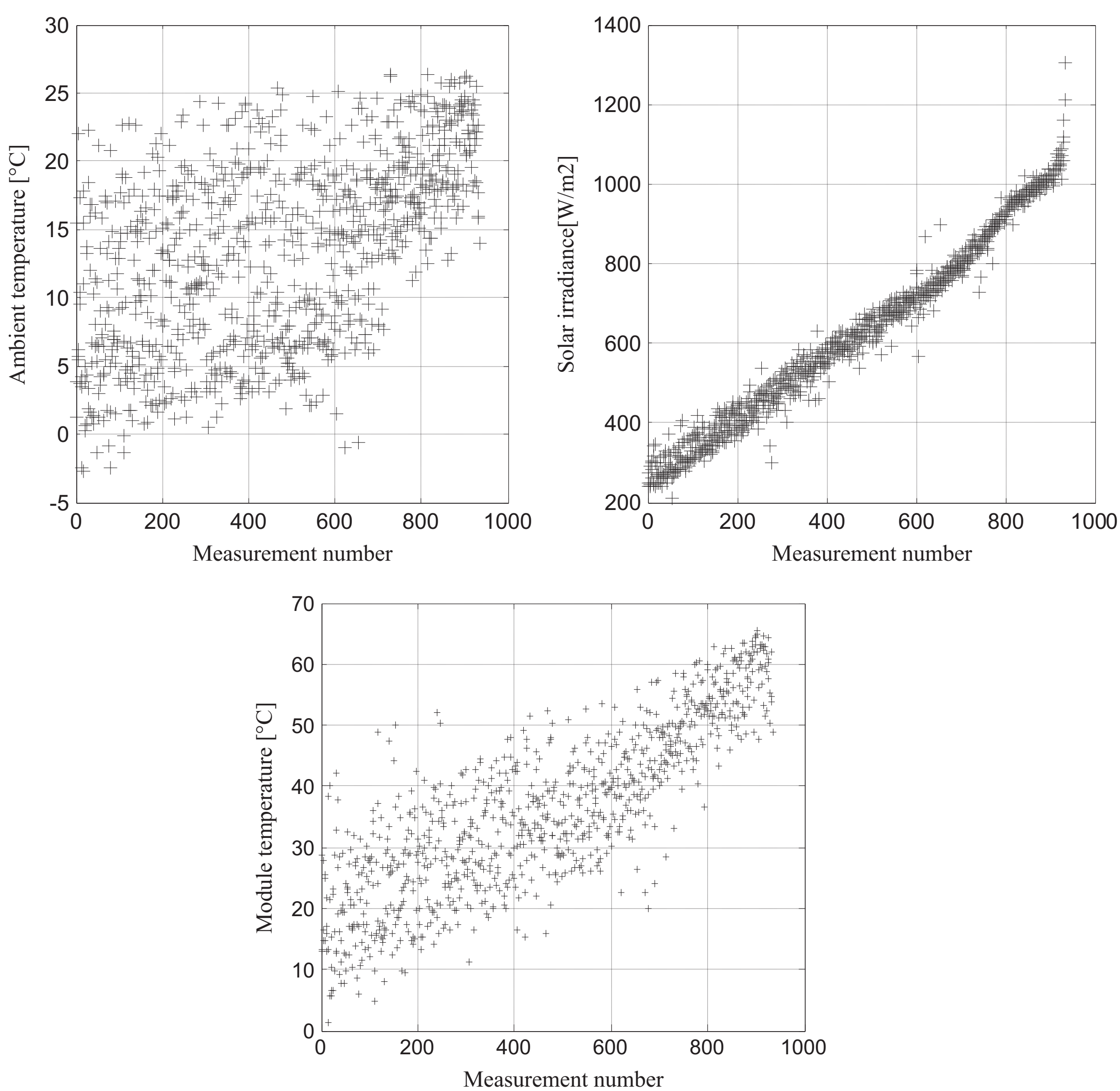

Fig. 4. Validation data of the CIS module.

scanner developed by Merten et al. [40] and fully described in [37]. Table 1 summarises the properties of the original database and the used database, while Figs. 3–5 illustrate the chosen *I–V* curves and the corresponding working conditions for the validation test of the three modules, monocrystalline silicon, CIS, and CdTe, respectively. This data was chosen to represent a broad range of working conditions (solar irradiance intensity and ambient temperature). In those samples the solar irradiance in the plane of the modules reached maximum values of approximately 1130 W/m^2, 1300 W/m^2, and 1200 W/m^2 for the monocrystalline silicon module, the CIS module, and the CdTe module, respectively. The modules maximum temperatures averaged between −2 °C and 63 °C for the monocrystalline silicon module, 1 °C and 66 °C for the CIS module, and between −2 °C and 61 °C for the CdTe one as illustrated in Figs. 3–5.

To verify the reliability of the B-model, we considered the following test procedure illustrated in Fig. 6. First, an important number of different working conditions from the measured database were selected on the basis of the solar irradiance intensity value. In the next step, the selected working conditions were used to calculate the *I–V* curves using the B-model. Finally, to assess the reliability of the model, the current difference between calculated and measured data was evaluated. This difference has been used to calculate three error metrics; the mean absolute error (*MAE*), the mean square error (*MSE*) and the root mean square error (*RMSE*)

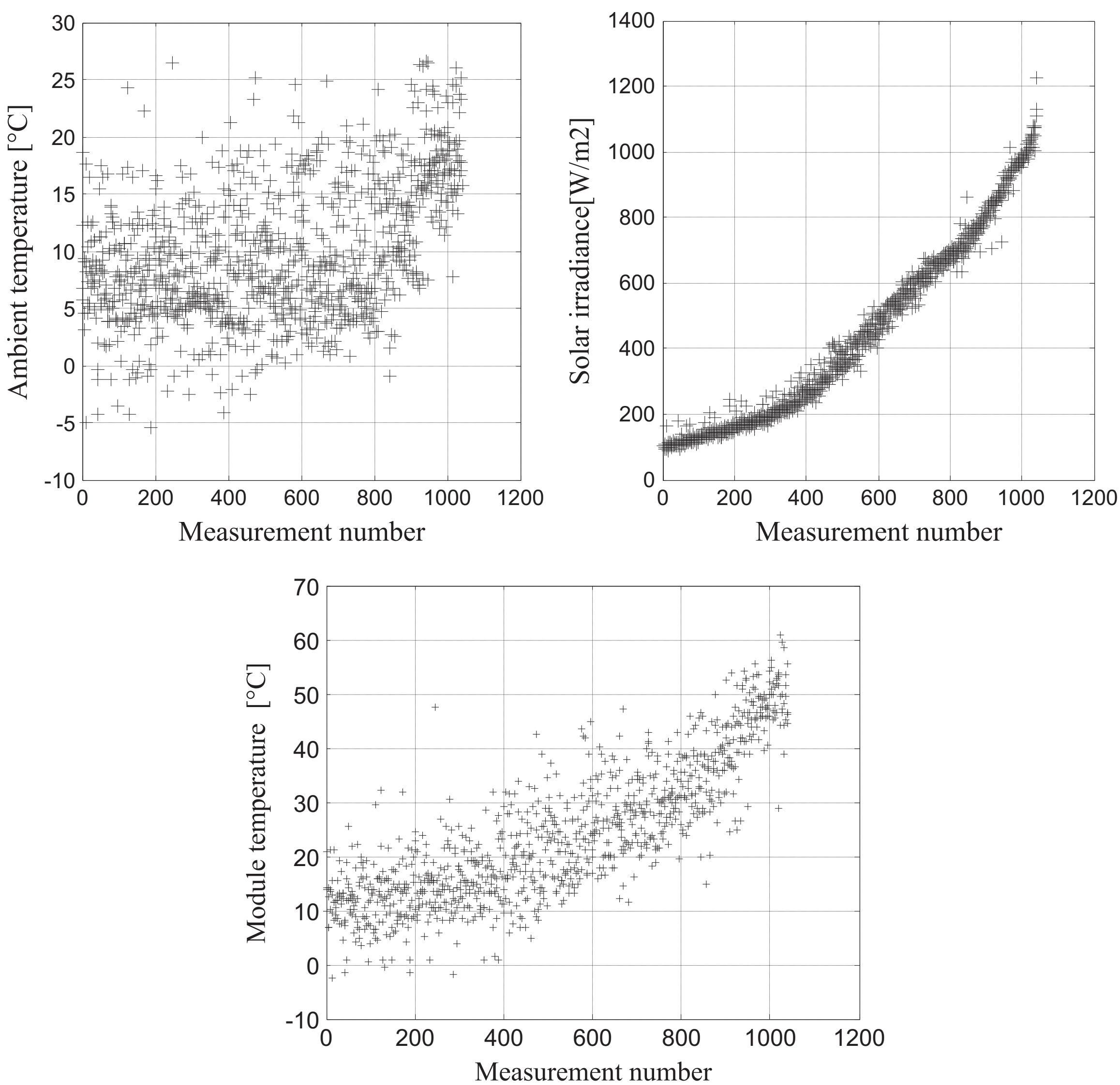

Fig. 5. Validation data of the CdTe module.

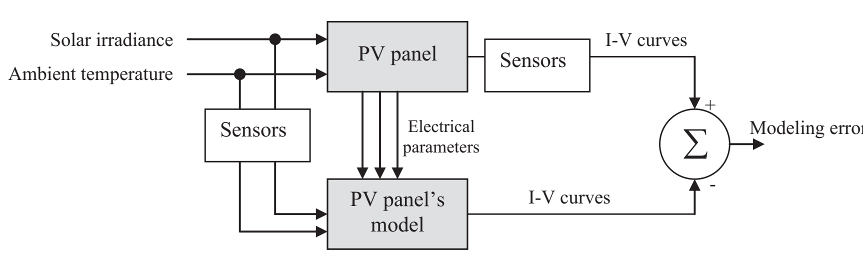

Fig. 6. Conceptual scheme of the experimental validation procedure.

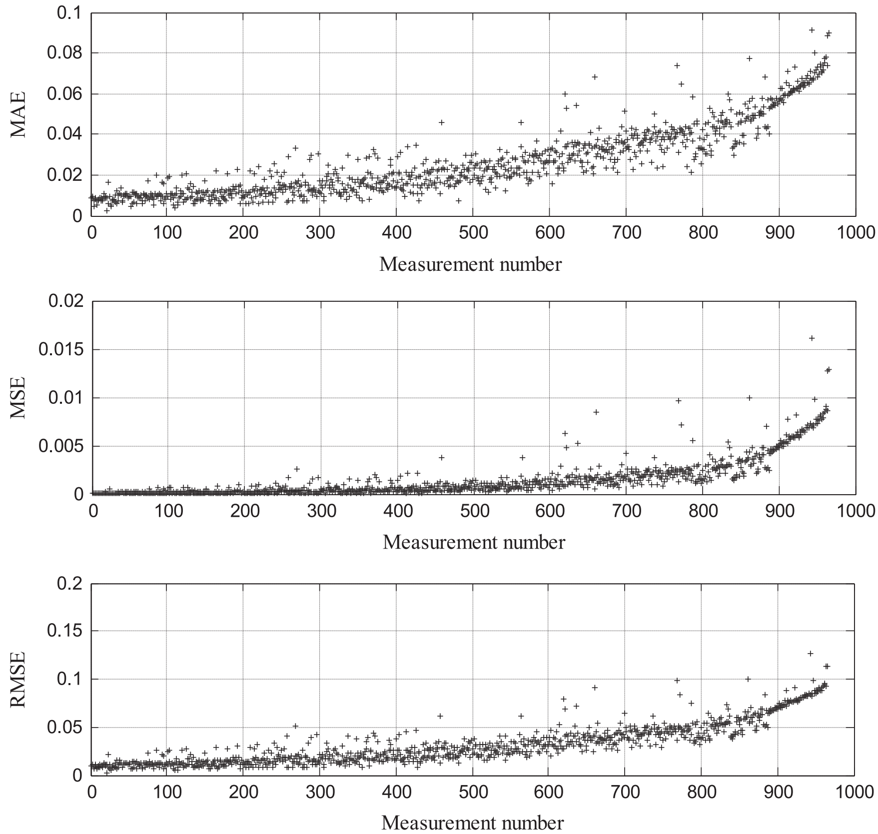

Fig. 7. Validation's errors of the monocrystalline silicon module.

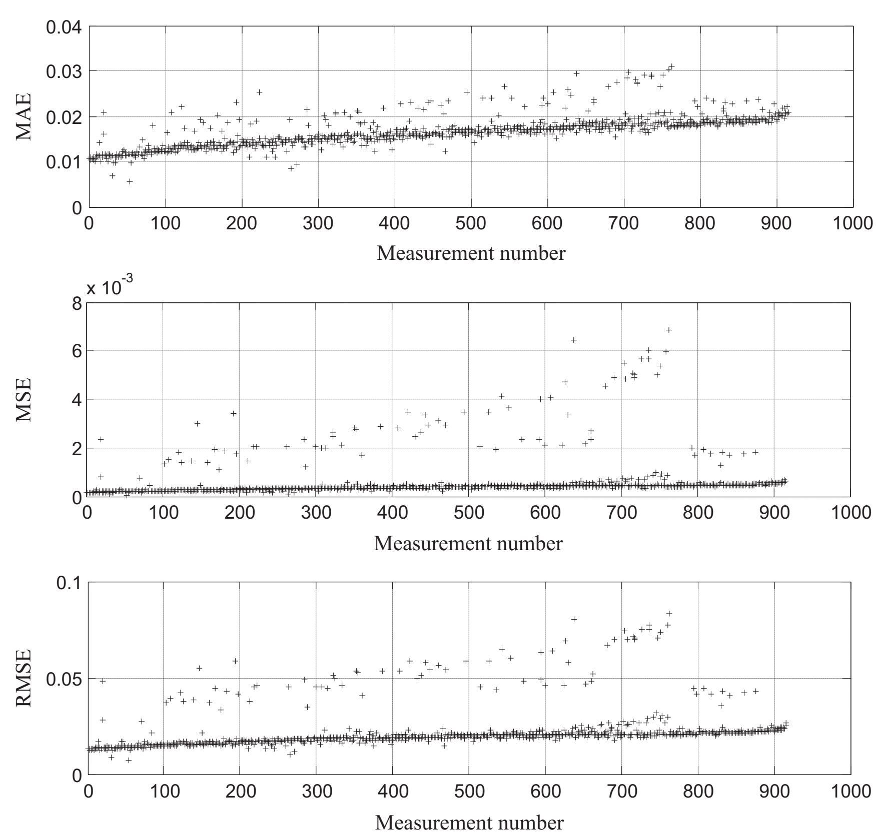

Fig. 8. Validation's errors of the CIS module.

noted by Eqs. (11)–(13) respectively, where I_m is the measured current and I_b is the calculated current using the B-model. *MAE* and *RMSE* have been used together to diagnose the variation in the errors in the large selected set of the validation samples. Note that the error metrics have been calculated first for each *I–V* curve for just exploring the effectiveness of the developed model for the different working conditions values. The number "100" in Eqs. (11) and (12) designates the number of measurements in each *I–V* curve.

$$MAE = \frac{\sum_{i=1}^{100} |I_m - I_b|}{100} \tag{11}$$

$$MSE = \frac{\sum_{i=1}^{100} (I_m - I_b)^2}{100} \tag{12}$$

$$RMSE = \sqrt{MSE} \tag{13}$$

The results of the comparison between measured and calculated data are illustrated in Figs. 7–12. First, the three error metrics for each *I–V* curve and for each PV module are presented. As can be seen, Figs. 7–9 show that *MAE* is less than 0.1 for the first module and less than 0.04 for the CIS and the CdTe modules, with a corresponding *RMSE* less than 0.15, 0.1 and 0.08. Note that the

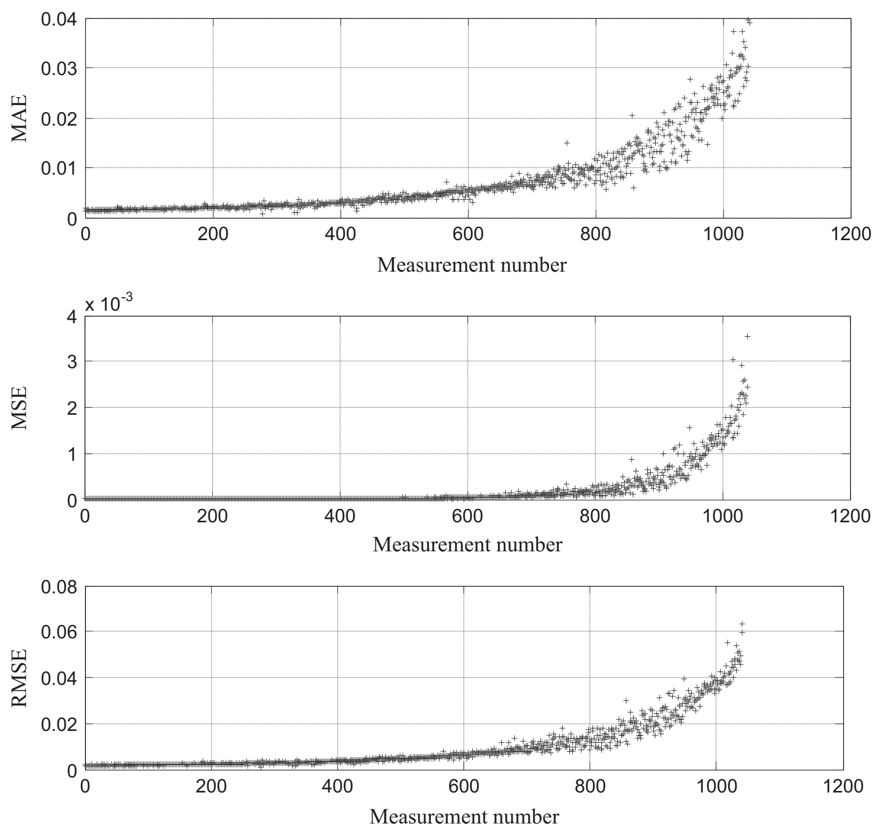

Fig. 9. Validation's errors of the CdTe module.

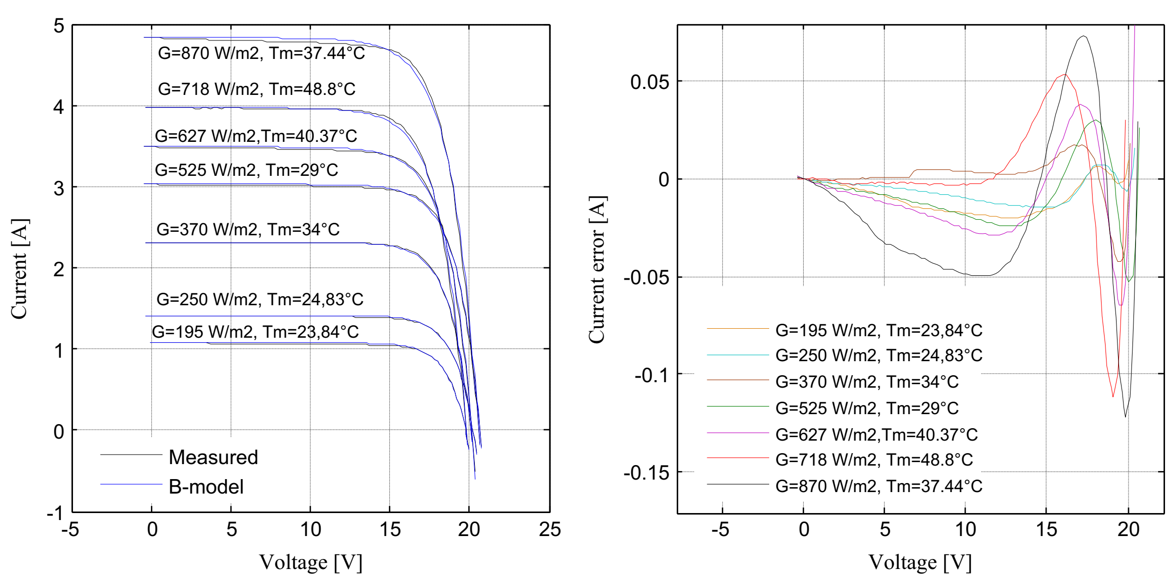

Fig. 10. Comparison between calculated (B-model) and measured current–voltage characteristics of the monocrystalline silicon module.

values of the three error metrics, calculated for all the measurements for all the samples according to Eqs. (14)–(16) and summarised by Table 2, can be qualified as satisfactory, knowing that N designates the number of I–V curves considered for the validation test which differs from one module to another as presented by Table 1. Next, in the interest of brevity, for each PV panel a few examples of measured and calculated I–V curves are shown purely for illustrative purposes. For this, different solar irradiance levels and module's temperatures are considered. As can be seen, the illustrations show a good relationship between the measured current and the current calculated with the B-model.

$$MAE = \frac{\sum_{n=1}^{N} \sum_{i=1}^{100} |I_m - I_b|}{N \cdot 100} \tag{14}$$

$$MSE = \frac{\sum_{n=1}^{N} \sum_{i=1}^{100} (I_m - I_b)^2}{N \cdot 100} \tag{15}$$

$$MSE = \sqrt{\frac{\sum_{n=1}^{N} \sum_{i=1}^{100} (I_m - I_b)}{N \cdot 100}} \tag{16}$$

5. Concrete example of use

This section presents a concrete application in which the improved model is used to overcome a technical problem. This model was used to simulate the real behaviour of a PV module in order to compare the efficiency of several Maximum Power Point Tracking (MPPT) algorithms in the absence of a dedicated experimental setup. As described in [41], a multi-crystalline silicone module's experimental database was used to design a model that is capable of simulating the module's behaviour continuously during the day time. In doing so, the initial

Table 2
The validation test: error metrics' values.

PV modules	Technology	MAE	MSE	RMSE
Mod1	Mono-crystalline silicon	0.0263	0.0015	0.0385
Mod2	CIS	0.0161	0.0006	0.0240
Mod3	CdTe	0.0071	0.0002	0.0146

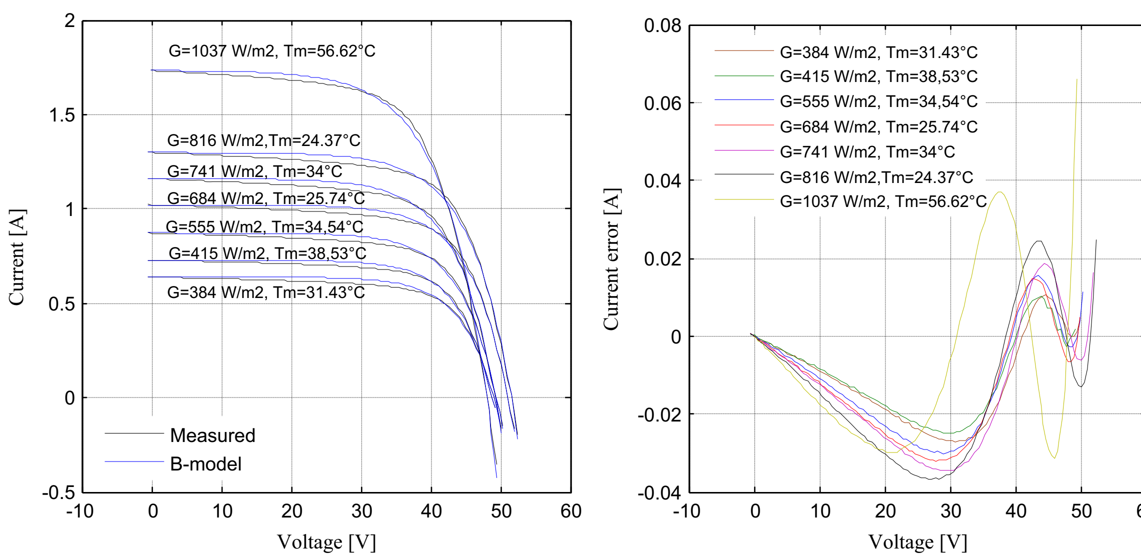

Fig. 11. Comparison between calculated (B-model) and measured current–voltage characteristics of the CIS module.

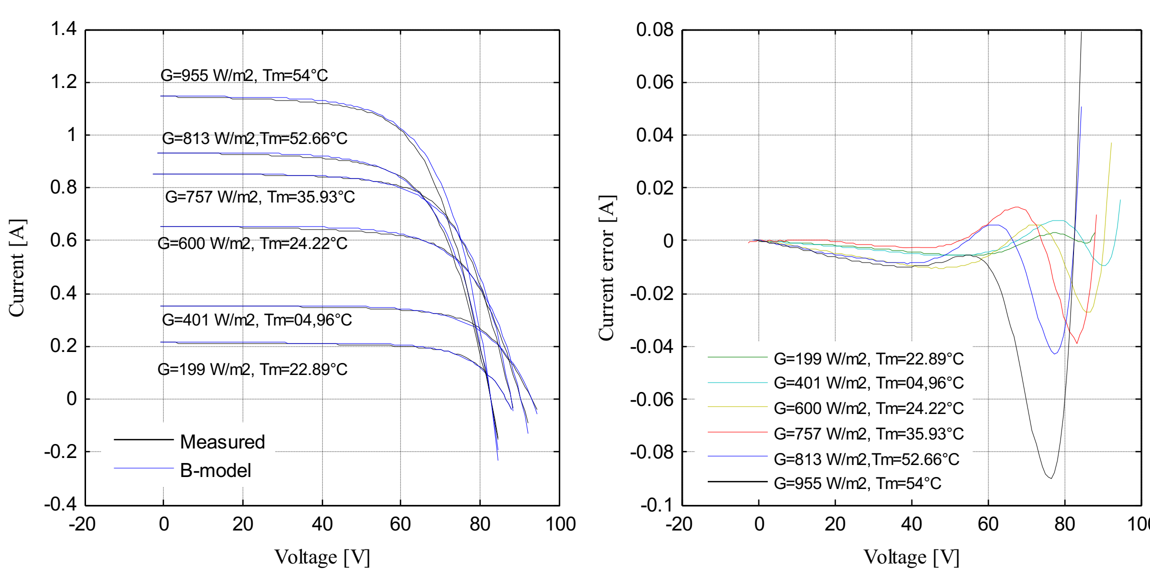

Fig. 12. Comparison between calculated (B-model) and measured current–voltage characteristics of the CdTe module.

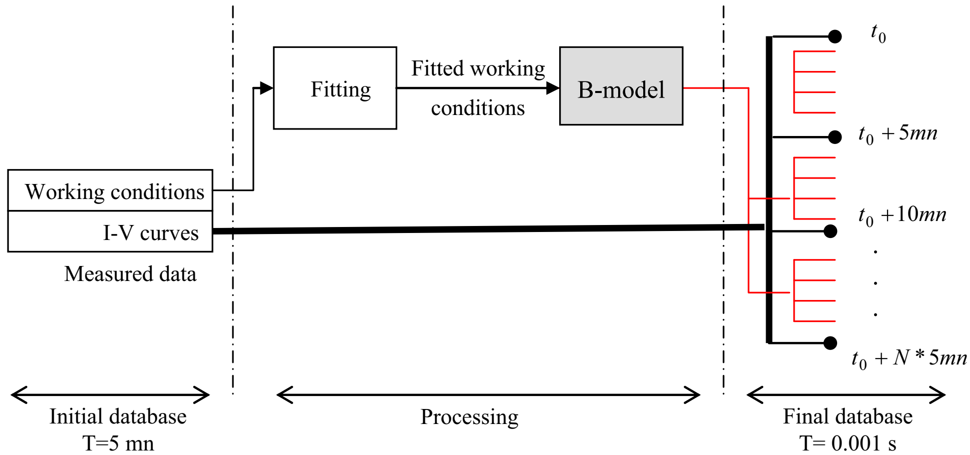

Fig. 13. Schematic diagram of B-model's use.

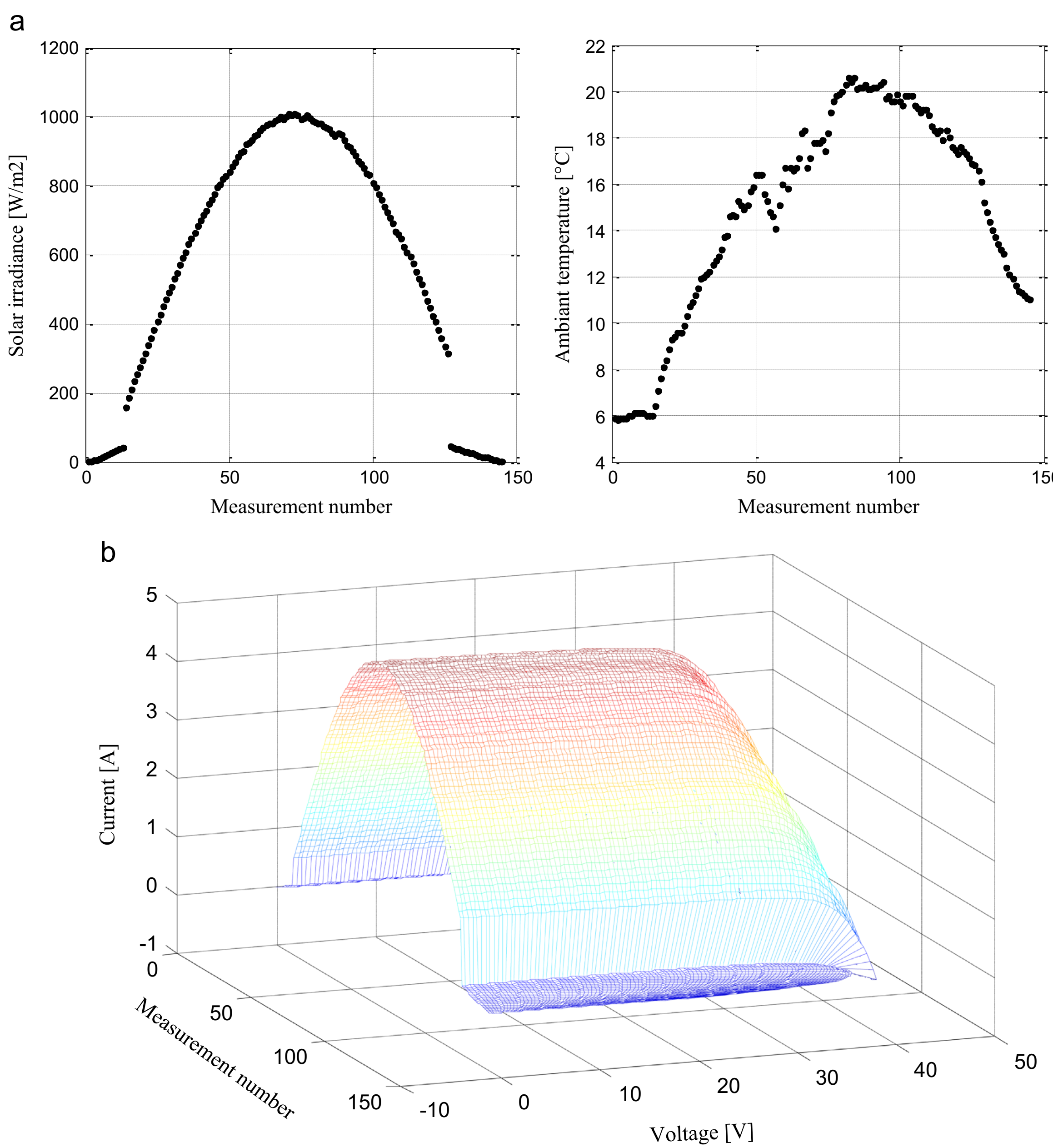

Fig. 14. Measured data during the day March 16, 2009 (polycrystalline silicon photovoltaic module).

database, which contains measurements that were collected every 5 min, could have been used to generate a new database. This simulates the module's outputs by using a shorter period as described by Fig. 13 which illustrates the schematic diagram of this example.

In our example, the continuous behaviour of the studied PV module is simulated based on the measured data. As shown in Fig. 14, the database corresponding to the date of March 29, 2009 is initially composed of 145 measuring times. Each measurement includes the working conditions (solar irradiance, ambient temperature) and the I–V curve. By using the B-model, for which the inputs are the fitted working conditions with 144,001 values for the same day by means of measuring period equal to 0.001 s, a new set of I–V curves is obtained as illustrated in Fig. 15. This new database has been used to simulate the continuous operation of the whole PV conversion system. This has allowed the study of several MPPT algorithms and the comparison of their efficiencies [41].

6. Conclusions

This study brings improvements to the previously developed behavioural model for PV modules, and provides easier use for photovoltaic systems simulations and study. In addition, the model was validated for three different module technologies.

To perform an experimental validation of the B-model, experimental data from three modules of different technologies: monocrystalline silicon, CIS and CdTe were utilised, knowing that the B-model was first developed based on a polycrystalline silicon module's experimental data. For this validation, a considerable number of working condition samples and the corresponding I–V curves were selected in such a way to represent a broad range of working conditions; from 200 W/m^2 to more than 1200 W/m^2 for the solar irradiance, and from 0 °C to more than 60 °C for the module temperature. The validation test showed satisfactory

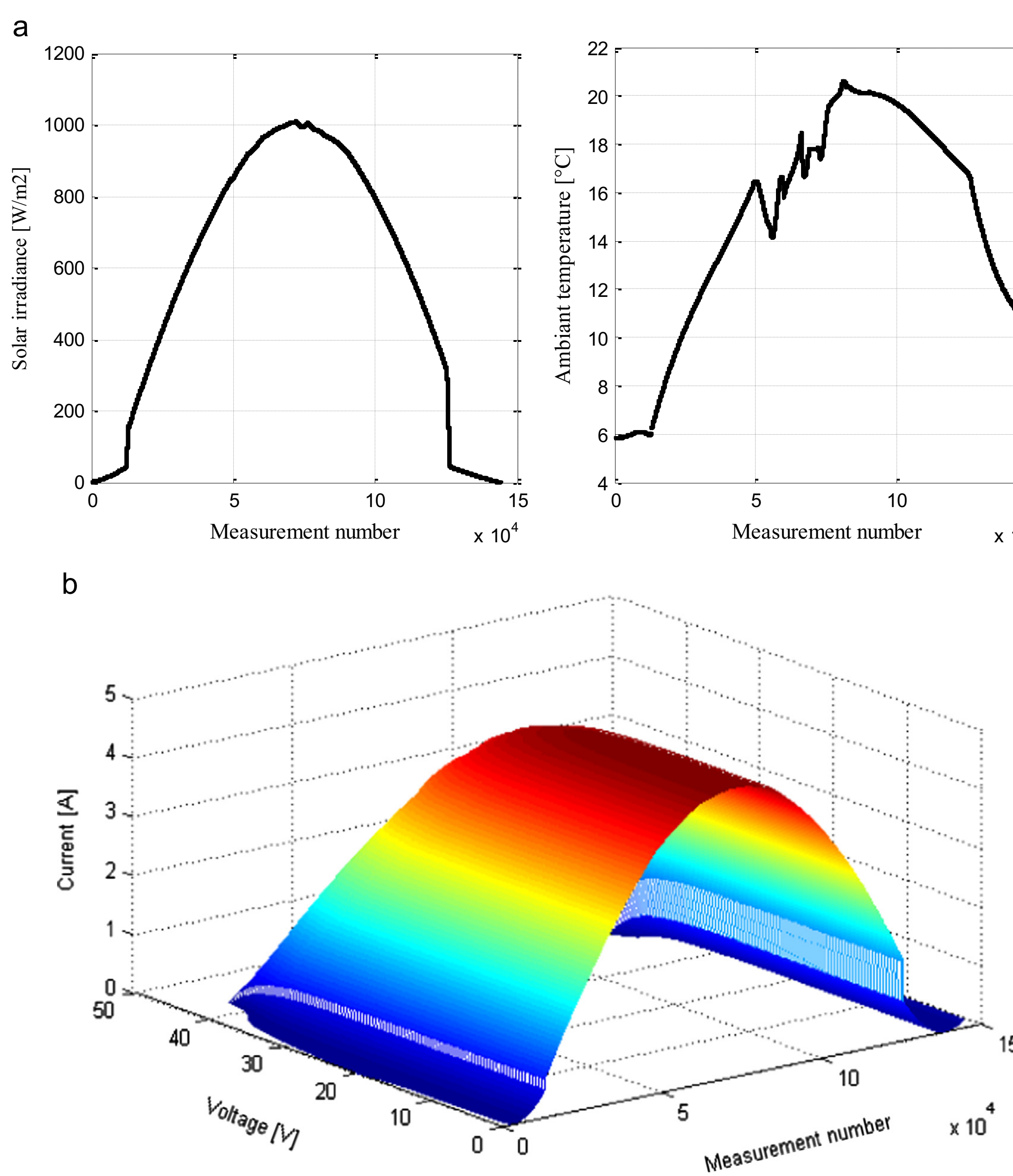

Fig. 15. Simulation data completed by using the B-model (polycrystalline silicon photovoltaic module).

results. In fact, an acceptable agreement between the measured *I*–*V* curves and the calculated *I*–*V* curves using the B-model was obtained. A concrete example of the use is presented and explained, and it shows that the B-model is efficient and very simple to use.

Further work is in progress to analyse the evolution of the maximum power point (MPP) properties. Particular interest is paid to understand the correlation between the value of the slope at the MPP (S_{MPP}), the ratio of the short circuit current, and the open circuit voltage. On this basis, a new expression for the constant voltage can be proposed in order to simplify its mathematical expression.

Acknowledgements

Part of this work was performed while the author was a researcher at INES (Institut National de l'Energie Solaire, France). The authors gratefully acknowledge the L2S (Laboratory for Solar Systems) researchers' team for their contribution to this work. Great thanks to Mr. Mohamed Bouali for his encouragement and understanding, also to Mr. Ben Fasano for his precious help.

References

[1] D.P. Gruber, G. Meinhardt, W. Papousek, Modelling the light absorption in organic photovoltaic devices, Sol. Energy Mater. Sol. Cells 87 (2005) 215–223.

[2] S. Michael, A novel approach for the modeling of advanced photovoltaic devices using the SILVACO/ ATLAS virtual wafer fabrication tools, Sol. Energy Mater. Sol. Cells 87 (2005) 771–784.

[3] J.F. Randall, J. Jacot, Is AM1.5 applicable in practice? Modelling eight photovoltaic materials with respect to light intensity and two spectra, Renew. Energy 28 (2003) 1851–1864.

[4] H. Takakura, Y. Hamakawa, Device simulation and modeling of microcrystalline silicon solar cells, Sol. Energy Mater. Sol. Cells 74 (2002) 479–487.

[5] Barbara Werner, WŁodzimierz KoŁodenny, Mariusz Prorok, Andrzej Dziedzic, Tadeusz Żdanowicz, Electrical modeling of CIGS thin-film solar cells working in natural conditions, Sol. Energy Mater. Sol. Cells 95 (2011) 2583–2587.

[6] M. Zeman, O. Isabella, S. Solntsev, K. Jäger, Modeling of thin-film silicon solar cells, Sol. Energy Mater. Sol. Cells 119 (2013) 94–111.

[7] F. Ghani, M. Duke, J. Carson, Numerical calculation of series and shunt resistance of a photovoltaic cell using the Lambert W-function: experimental evaluation, Sol. Energy 87 (2013) 246–253.

[8] H. Pfleiderer, B. Bullemer, Multi-region solar cell modeling, Sol. Energy Mater. Sol. Cells 46 (1997) 17–27.

[9] Ana-Maria Teodoreanu, Caspar Leendertz, Tobias Sontheimer, Bernd Lars Korte, An effective medium approach for modeling polycrystalline silicon thin film solar cells, Sol. Energy Mater. Sol. Cells 117 (2013) 152–160.

[10] Nowshad Amin, Kamaruzzaman Sopian, Makoto Konagai, Numerical modeling of CdS/CdTe and CdS/CdTe/ZnTe solar cells as a function of CdTe thickness, Sol. Energy Mater. Sol. Cells 91 (2007) 1202–1208.

[11] Marika Edoff Ulf Malm, 2D device modeling and finite element simulations for thin-film solar cells, Sol. Energy Mater. Sol. Cells 93 (2009) 1066–1069.

[12] W. De Soto, S.A. Klein, W.A. Beckman, Improvement and validation of a model for photovoltaic array performance, Sol. Energy 80 (2006) 78–88.

[13] Jee-Hoon Jung, Shehab Ahmed, Real-time simulation model development of single crystalline photovoltaic panels using fast computation methods, Sol. Energy 86 (2012) 1826–1837.

[14] Rob W. Andrews, Andrew Pollard, Joshua M. Pearce, Improved parametric empirical determination of module short circuit current for modelling and optimization of solar photovoltaic systems, Sol. Energy 86 (2012) 2240–2254.

[15] Hongmei Tian, Fernando Mancilla-David, Kevin Ellis, Eduard Muljadi, Peter Jenkins, A cell-to-module-to-array detailed model for photovoltaic panels, Sol. Energy 86 (2012) 2695–2706.

[16] Ali Naci Celik, Nasır Acikgoz, Modelling and experimental verification of the operating current of mono-crystalline photovoltaic modules using four- and five-parameter models, Appl. Energy 84 (2007) 1–15.

[17] Valerio LoBrano, Aldo Orioli, Giuseppina Ciulla, Alessandra Di Gangi, An improved five-parameter model for photovoltaic modules, Sol. Energy Mater. Sol. Cells 94 (2010) 1358–1370.

[18] Valerio LoBrano, Aldo Orioli, Giuseppina Ciulla, On the experimental validation of an improved five-parameter model for silicon photovoltaic modules, Sol. Energy Mater. Sol. Cells 105 (2012) 27–39.

[19] M.U. Siddiqui, M. Abido, Parameter estimation for five- and seven-parameter photovoltaic electrical models using evolutionary algorithms, Appl. Soft Comput. 13 (2013) 4608–4621.

[20] T. Huld, G. Friesen, A. Skoczek, R.P. Kenny, T. Sample, M. Field, E.D. Dunlop, A power-rating model for crystalline silicon PV modules, Sol. Energy Mater. Sol. Cells 95 (2011) 3359–3369.

[21] E. Skoplaki, J.A. Palyvos, Operating temperature of photovoltaic modules: a survey of pertinent correlations, Renew. Energy 34 (2009) 23–29.

[22] D.L. King, P.E. Eckert, Characterizing (rating) the performance of large photovoltaic arrays for all operating conditions, in: Proceedings of the 25th IEEE Photovoltaic Specialists Conference, 1996, pp. 1385–1388.

[23] J.P. Kim, H. Lim, J.H. Song, Y.J. Chang, C.H. Jeon, Numerical analysis on the thermal characteristics of photovoltaic module with ambient temperature variation, Sol. Energy Mater. Sol. Cells 95 (2011) 404–407.

[24] M. Piliougine, D. Elizondo, L. Mora-Lopez, M. Sidrach-de-Cardona, Multilayer perceptron applied to the estimation of the influence of the solar spectral distribution on thin-film photovoltaic modules, Appl. Energy 112 (2013) 610–617.

[25] A. Ravi, P.S. Manoharan, J. Vijay Anand, Modeling and simulation of three phase multilevel inverter for grid connected photovoltaic systems, Sol. Energy 85 (2011) 2811–2818.

[26] V. Fernao Pires, J.F. Martins, C. Hao, Dual-inverter for grid-connected photovoltaic system: modeling and sliding mode control, Sol. Energy 86 (2012) 2106–2115.

[27] M. Valan Rajkumar, P.S. Manoharan, A. Ravi, Simulation and an experimental investigation of SVPWM technique on a multilevel voltage source inverter for photovoltaic systems, Electr. Power Energy Syst. 52 (2013) 116–131.

[28] N. Patcharaprakiti, K. Kirtikara, V. Monyakul, D. Chenvidhya, J. Thongpron, A. Sangswang, B. Muenpinij, Modeling of single phase inverter of photovoltaic system using Hammerstein–Wiener nonlinear system identification, Curr. Appl. Phys. 10 (2010) 532–536.

[29] J.B. Copetti, F. Chenlo, Lead/acid batteries for photovoltaic applications. Test results and modelling, J. Power Sources 47 (1994) 109–118.

[30] J.N. ROSS, T. Markvart, W. He, Modelling battery charge regulation for a stand-alone photovoltaic system, Sol. Energy 69 (2000) 181–190.

[31] N. Achaibou, M. Haddadi, A. Malek, Lead acid batteries simulation including experimental validation, J. Power Sources 185 (2008) 1484–1491.

[32] P.E. Campana, H. Li, J. Yan, Dynamic modelling of a PV pumping system with special consideration on water demand, Appl. Energy 112 (2013) 635–645.

[33] M. Jafar, A model for small-scale photovoltaic solar water pumping, Renew. Energy 19 (2000) 85–90.

[34] A. Hadj Arab, M. Benghanem, F. Chenlo, Motor-pump system modelization, Renew. Energy 31 (2006) 905–913.

[35] J. Bai, S. Liu, Y. Hao, Z. Zhang, M. Jiang, Y. Zhang, Development of a new compound method to extract the five parameters of PV modules, Energy Convers. Manag. 79 (2014) 294–303.

[36] G. Ciulla, V. LoBrano, V. Di Dio, G. Cipriani, A comparison of different one-diode models for the representation of *I*–*V* characteristic of a PV cell, Renew. Sustain. Energy Rev. 32 (2014) 684–696.

[37] B. Amrouche, A. Guessoum, M. Belhamel, A simple behavioural model for solar module electric characteristics based on the first order system step response for MPPT study and comparison, Appl. Energy 91 (2012) 395–404.

[38] B. Amrouche, L. Sicot, A. Guessoum, M. Belhamel, Experimental analysis of the maximum power point's properties for four photovoltaic modules from different technologies: monocrystalline and polycrystalline silicon, CIS and CdTe, Sol. Energy Mater. Sol. Cells 118 (2013) 124–134.

[39] J. Merten, J. Andreu, Clear separation of seasonal effects on the performance of amorphous silicon solar modules by outdoor *I*/*V*-measurements, Sol. Energy Mater. Sol. Cells 52 (1998) 11–25.

[40] J. Merten, L. Sicot, Y. Delesse, A. Guérin de Montgareuil, Outdoor evaluation of the energy production of different module technologies, in: Proceedings of the 23rd European Photovoltaic Solar Energy Conference Exhibition, 2008, pp. 2841– 2845.

[41] B. Amrouche, Contribution au développement d'une nouvelle méthode MPPT basée sur les concepts de l'intelligence artificielle pour les systèmes photovoltaïques (Ph.D. thesis), University Saad Dahleb de Blida, Algeria, 2013.